Toxicologic Pathology, 34:364–372, 2006

ISSN: 0192-6233 print / 1533-1601 online
DOI: 10.1080/01926230600815122

Welding Fume Exposure and Associated Inflammatory and Hyperplastic Changes in the Lungs of Tumor Susceptible A/J Mice

CLAUDIA SOLANO-LOPEZ,* PATTI C. ZEIDLER-ERDELY,* ANN F. HUBBS, STEVEN H. REYNOLDS, JENNY R. ROBERTS, MICHAEL D. TAYLOR, SHIH-HOUNG YOUNG, VINCENT CASTRANOVA, AND JAMES M. ANTONINI

Health Effects Laboratory Division, National Institute for Occupational Safety and Health, Morgantown, WV 26505, USA

ABSTRACT

It has been suggested that welding fume (WF) exposure increases lung cancer risk in welders. Epidemiology studies have failed to conclude that WF alone causes lung cancer and animal studies are lacking. We examined the course of inflammation, damage, and repair in the lungs of A/J mice, a lung tumor susceptible strain, caused by stainless steel WF. Mice were exposed by pharyngeal aspiration to 40 mg/kg of WF, silica, or saline. Bronchoalveolar lavage (BAL) was performed 24 hours, 1 and 16 weeks to assess lung injury and inflammation and histopathology was done 1, 8, 16, 24, and 48 weeks postexposure. Both exposures increased inflammatory cells, lactate dehydrogenase and albumin at 24 hr and 1 week. At 16 weeks, these parameters remained elevated in silica-exposed but not WF-exposed mice. Histopathologic evaluation at 1 week indicated that WF induced bronchiolar epithelial hyperplasia with associated cellular atypia, alveolar bronchiolo-alveolar hyperplasia (BAH) in peribronchiolar alveoli, and peribronchiolar lymphogranulomatous inflammation. Persistent changes included foci of histiocytic inflammation, fibrosis, atypical bronchiolar epithelial cells, and bronchiolar BAH. The principle changes in silica-exposed mice were histiocytic and suppurative inflammation, fibrosis, and alveolar BAH. Our findings that WF causes persistent bronchiolar and peribronchiolar epithelial changes, suggest a need for studies of bronchiolar changes after WF exposure.

Keywords. bronchoalveolar hyperplasia; lung inflammation; silica; strain A mice; welding fume.

INTRODUCTION

It is estimated that more than 2,000,000 workers worldwide perform welding as part of their work duties. Welding processes produce airborne particulate matter that is comprised of a complex mixture of metal oxides (Antonini, 2003). The metal composition of the generated fume is mostly derived from the welding electrode or wire consumed during the process. Welding processes that use stainless steel wire can produce fumes that contain metals known to be carcinogenic to humans, such as chromium (Cr) and nickel (Ni).

One potential health outcome associated with welding fume (WF) exposure is the development of lung cancer. The International Agency for Research on Cancer (IARC) has concluded that WFs were "possibly carcinogenic" to humans, despite the fact that the finding was based on limited evidence in humans and inadequate evidence in laboratory animals (IARC, 1990). Several epidemiology studies suggest exposure to WFs is associated with an increased incidence of lung cancer (Becker, 1999; Moulin 1997; Simonato et al., 1991). However, other studies have not observed this elevated risk (Danielsen et al., 2000; Hansen et al., 1996; Steenland et al., 1991). Workplace setting, asbestos exposure, and a higher smoking prevalence among welders all may contribute to this increased risk which makes a clear association with WF difficult (Hansen et al., 1996; Sterling and Wenkham, 1976).

The purpose of this pilot study was to characterize the progression of lung injury and repair following exposure to WF, via pharyngeal aspiration, in A/J mice, a lung tumor susceptible mouse strain. This particular model offers advantages in contrast to other rodent models employed previously. First, mouse pharyngeal aspiration is a simple, well-established and efficient method used to expose the lower airways of the lung to particulates (Rao et al., 2003). Second, the availability of mouse strains that differ in their tumor susceptibility allows for potential strain comparisons in future studies. A/J mice, in particular, are classified as being highly susceptible to spontaneous and chemical-induced lung tumors as compared to the essentially resistant mouse strain, C57BL/6J (Shimkin and Stoner, 1975). Genetic evidence for an increased susceptibility to lung tumorigenesis was verified through different strain crosses that allowed the mapping in A/J mice of the pulmonary adenoma susceptibility 1 (*Pas1*) locus, the primary locus responsible for predisposition to lung cancer in mice (Gariboldi et al., 1993). The presence of a susceptibility allele($Pas1^s$), along with other lung cancer modifier loci, or a resistant allele ($Pas1^r$) at the *Pas1* locus determines mouse lung tumor susceptibility (Malkinson, 1989; Manenti et al., 1996, 1999). Finally, the lung tumors in susceptible mouse strains exhibit many morphological, histopathological, and molecular similarities to human pulmonary adenocarcinomas, making them a unique model for lung cancer research (Van Zandwijk et al., 1995; Malkinson, 1998; Meuwissen and Berns, 2005).

Address correspondence to: James M. Antonini, Health Effects Laboratory Division, National Institute for Occupational Safety and Health, 1095 Willowdale Road (M/S 2015) Morgantown, WV 26505, USA; e-mail: jga6@cdc.gov

*Denotes equal contribution to this work. The findings and conclusions in this report are those of the author(s) and do not necessarily represent the views of the National Institute for Occupational Safety and Health.

Abbreviations: ANOVA: analysis of variance; BAL: bronchoalveolar lavage; BAH: bronchiolo-alveolar hyperplasia; Cr: chromium; GMA- MS: gas metal arc-mild steel; GMA- SS; gas metal arc-stainless steel; H&E: hematoxylin and eosin; LDH: lactate dehydrogenase; MMA- SS; manual metal arc-stainless steel; Ni: nickel; PBS: phosphate-buffered saline; SE: standard error; WF: welding fume.

This study addresses lung histopathological changes as well as bronchoalveolar lavage (BAL) indices of cellular infiltration, damage, and toxicity in the A/J mouse exposed to manual metal arc-stainless steel (MMA-SS) WF by pharyngeal aspiration. These preliminary data will serve as a basis for testing of future hypotheses of WF-induced lung tumorigenesis in mice. A comparison to crystalline silica (α-quartz), a particle known to cause pulmonary inflammation and fibrosis, is made.

Materials and Methods

Welding Fume Collection and Characterization. The collection and characterization of the MMA-SS WF was previously described by Antonini et al. (1999). The WF was comprised of Fe, Cr, Mn, and Ni at concentrations of 33.4, 23.2, 13.6, and 0.3 μg/mg total weight of all metals measured, respectively. In addition, the particle size of the fume was found to be of respirable size with a count mean diameter of <2.0 μm.

Laboratory Animals. Male A/J mice, 6 weeks of age with an average weight of 20.6 ± 2.0 g, were purchased from Jackson Laboratories (Bar Harbor, ME) and housed in an AAALAC-accredited, specific pathogen-free, environmentally controlled facility. All mice were free of endogenous viral pathogens, parasites, mycoplasmas, Helicobacter, and CAR Bacillus. Mice were separately housed in ventilated cages and provided HEPA-filtered air under a controlled light cycle (12-hour light/12 hr dark) at a standard temperature (22–24°C). Animals were acclimated to the animal facility for one week after arrival and allowed access to a conventional diet (6% Irradiated NIH-31 Diet, Harlan Teklad, Madison, WI) and tap water ad libitum. All procedures were performed using protocols approved by the National Institute for Occupational Safety and Health Institutional Animal Care and Use Committee.

Experimental Design. A/J mice were exposed by pharyngeal aspiration to a suspension of the MMA-SS WF, silica (pneumotoxic particle control; 98.5% crystalline α-quartz, particle diameter <5.0 μm, U.S. Silica Co., Berkeley Springs, WV), or sterile Ca^{+2} and Mg^{+2}-free phosphate-buffered saline (PBS, pH 7.4; vehicle control). A bolus dose of 40 mg/kg was used for each particle based upon a C57BL/6J mouse model of lung silicosis that revealed significant lung damage and fibrosis at 42 days postexposure (Zeidler et al., 2004). This dose would be representative of a cumulative exposure in the workplace. See Table 1 for the details of the experimental design. At 24 hours, 1 week, and 16 weeks after treatment, BAL was performed on at least four randomly selected mice from each group to assess lung injury and inflammation. At 1, 8, 16, 24, and 48 week postexposure, mice ($n = 2$–4/group) were sacrificed and the lungs prepared for histopathological examination using light microscopy. It is important to note that 2 mice from both the silica and the WF groups did not survive the 48-week period. Upon necropsy, it was concluded that the deaths were not related to the exposures and no tumors or gross abnormalities were found. A complete pathological analysis could not be performed on these animals due to the lack of lung inflation-fixation upon death.

Table 1.—Experimental design

Time point	Bronchoalveolar lavage: cell differential lung injury	Histopathological analysis
24 hr	PBS, Si, WF: n = 7/group	n.d.
1 wk	PBS, Si, WF: n = 6/group	PBS, Si, WF: n = 2/group
8 wk	n.d.	PBS, Si, WF: n = 4/group
16 wk	PBS, Si, WF: n = 4/group	PBS, Si, WF: n = 4/group
24 wk	n.d.	PBS, Si, WF: n = 4/group
48 wk	n.d.	PBS, Si, WF: n = 4/group*

Note: n.d. is not determined; PBS is phosphate-buffered saline control; Si is silica; WF is welding fume.

*Premature deaths, unrelated to exposure, occurred in both WF and Si groups. The 48-week time point includes an n = 2 for these groups.

Animal Treatment. The MMA-SS WF and silica samples were suspended in sterile PBS and sonicated for 1 min with a Sonifier 450 Cell Disruptor (Branson Ultrasonics, Danbury, CT, USA). Mice were given a single 40 mg/kg dose of MMA-SS WF or silica by pharyngeal aspiration as described by Rao et al. (2003). Control mice were administered sterile PBS by the same method. Aspiration volumes were between 20–30 μl per mouse. Briefly, each mouse was anesthetized with a subcutaneous injection of a ketamine (Phoenix Pharmaceutical Inc., St. Joseph, MO)-xylazine mixture (50 and 2 mg/kg, respectively). The mouse was then placed in a supine position on a slanted board, hung from its top incisors on a rubber band. The tongue was completely extended with forceps and the solution was placed at the back of the throat. The mouse remained on the board until a few deep breaths were heard, indicating successful aspiration, then returned to its cage to recover (approximately 15–25 minutes).

Body weight changes of all mice were determined weekly to assess general health status (data not shown). None of the exposures had a significant effect on body weight compared to the saline controls throughout the 48-week period.

Bronchoalveolar Lavage. To assess pulmonary injury and inflammation, BAL of the whole lungs was performed at 24 hours, 1 week, and 16 weeks postexposure. Mice were weighed and euthanized with an intraperitoneal injection of sodium pentobarbital (>100 mg/kg body weight, Butler Co., Columbus, OH). The trachea was cannulated with a blunted 22-gauge needle, and BAL was carried out using cold PBS. For the initial step, 0.9 ml of sterile PBS was instilled into the lung; the solution was allowed to remain in the lungs for 30 seconds, while massaging the thorax. After 30 sec, the solution was withdrawn and re-instilled into the lungs, followed by the immediate retrieval of the fluid. This constituted the first fraction of the BAL. Eleven subsequent lavages (0.9 ml/instillate) were done and collected into a 50 ml centrifuge tube, representing the second fraction. The fractions were preserved on ice until all the animals of the time point were sacrificed. The BAL samples were centrifuged ($500 \times g$, 10 minutes, 4°C), and the acellular fluid from the first fraction was used for the determination of lung damage, whereas the supernatant of the second fraction was discarded. The cell pellets from both fractions were combined and resuspended in 1 ml of PBS. Total cell numbers were determined using a Coulter Multisizer (Coulter Electronics, Hialeah, FL) and differential cell counts were performed via cytospin (Shandon Cytospin II, Shandon Inc., Pittsburgh, PA) and Leukostat

stain (Fisher Scientific, Pittsburgh PA) to determine the number of alveolar macrophages and neutrophils.

Lung Injury. Albumin, an index of increased permeability of the alveolar-capillary barrier, and lactate dehydrogenase (LDH) activity, an indicator of general cytotoxicity, were measured in the first fraction BAL supernatant. Albumin concentration was determined colorimetrically at 628 nm based on albumin binding to bromocresol green, using an albumin BCG diagnostic kit (Sigma Chemical Co., St. Louis, MO, USA). LDH activity was determined by measuring the oxidation of lactate to pyruvate coupled with the formation of NADH at 340 nm. Measurements were performed with a COBAS MIRA auto-analyzer (Roche Diagnostic Systems, Montclair, NJ, USA).

Histopathology. Whole lungs from selected animals from each group were excised, completely inflated and fixed with 10% neutral buffered formalin for 24 hours. Lungs were embedded in paraffin and sectioned in 5 μm slices onto microscope slides. Left and right lung lobe sections were stained with hematoxylin and eosin (H&E). The left lung lobes from the 1, 8, 16, 24 and 48 week group were also stained with Masson's trichrome to assess fibrosis. Morphologic changes in tissue sections were evaluated in a blinded fashion by a board-certified veterinary pathologist and semiquantitatively scored. Pathology scores for each section were the sum of the distribution (0 = none, 1 = focal, 2 = locally extensive, 3 = multifocal, 4 = multifocal and coalescent, 5 = diffuse) and severity (0 = none, 1 = minimal, 2 = mild, 3 = moderate, 4 = marked, 5 = diffuse) as previously described (Hubbs et al., 1997). Histopathological alterations were diagnosed and scores were recorded for the most common types of morphologic changes seen in this study: (1) inflammation, (2) lymphoid hyperplasia, (3) bronchiolar type bronchiolo-alveolar hyperplasia (bronchiolar BAH), (4) alveolar type bronchiolo-alveolar hyperplasia (alveolar BAH) and (5) hyperplasia, epithelial with cellular atypia in bronchioles and (6) pulmonary fibrosis. Hyperplastic lesions were classified as previously described (Dungworth et al., 2001).

The final pathology score for inflammatory and proliferative alterations were the mean of the scores for the left and the right lung lobes of each mouse (n = 4/group) and were statistically analyzed for the 8, 16, and 24 week time points. Final scores for the 1-week groups (n = 2/group) were also calculated but not statistically analyzed. Fibrosis scores were calculated from the score of the left lung lobe and statistically analyzed at the 8, 16, and 24 week time points (Table 4).

Statistical Analysis. Results are expressed as means ± standard error (SE). Statistical analyses were applied to the data in Tables 2, 3, and 4 using a 2-way analysis of variance (ANOVA) and the Fischer's Least Significance Difference post-hoc test (SAS, Inc., Belmont, CA). For all analyses, the criterion of significance was $p < 0.05$.

RESULTS

Bronchoalveolar Lavage and Indices of Lung Injury. To determine cellular infiltration into the lung, BAL cell counts and differentials were performed at 24 hours, 1 week, and 16 weeks postexposure (Table 2). Total BAL cell yield increased versus control following WF or silica exposure at all time points measured, with the 1 week and 16 weeks achieving statistical significance.

TABLE 2.—Bronchoalveolar lavage cell differentials

Treatment	Total Cells (10^6)	Macrophages (10^6)	Neutrophils (10^6)
24 hr			
PBS	3.42 ± 0.96	3.40 ± 0.95	0.01 ± 0.00
Si	6.98 ± 2.36	2.82 ± 0.97	4.02 ± 1.52[a]
WF	3.59 ± 0.89	1.91 ± 0.51	1.62 ± 0.43[a]
1 wk			
PBS	1.41 ± 0.29	1.36 ± 0.28	0.00 ± 0.00
Si	2.43 ± 0.24[a]	1.68 ± 0.12	0.72 ± 0.14[b]
WF	2.55 ± 0.23[a]	2.11 ± 0.21	0.27 ± 0.04[a]
16 wk			
PBS	1.27 ± 0.13	1.23 ± 0.14	0.01 ± 0.01
Si	1.91 ± 0.03[a]	1.46 ± 0.04	0.38 ± 0.03[b]
WF	2.35 ± 0.40[a]	2.23 ± 0.37	0.04 ± 0.01

Note: Values are means ± SE (n ≥ 4), PBS is phosphate-buffered saline control; Si is silica; WF is welding fume.
[a] Significantly greater than PBS at corresponding time point ($p < 0.05$).
[b] Significantly greater than PBS and WF groups at corresponding time point ($p < 0.05$).

No significant difference in macrophage number was found among the groups at any time points. The neutrophil response for both the WF and silica-exposed mice was significantly elevated versus control at 24 hours and 1 week. By 16 weeks, this response had returned to control in the WF group but persisted in the silica-exposed animals. Silica exposure in A/J mice elicited a statistically significant neutrophil increase compared to WF, approximately 2.6- and 9.5-fold greater at 1 week and 16 weeks, respectively.

Lung cytotoxicity and air-blood barrier leakage were measured as LDH and albumin, respectively, in the first fraction BAL supernatant at 24 hours, 1 week, and 16 weeks post-exposure. At 24 hours and 1 week, both WF and silica-exposed mice exhibited significant lung cytotoxicity and air-blood barrier leakage compared to saline control (Table 3). By 16 wk, these parameters were no longer increased compared to control in the WF group. However, both LDH activity and albumin content remained statistically elevated in the silica-exposed mice compared to saline control.

Lung Histopathology. At 1, 8, 16, and 24 weeks, histopathology scores were determined for lungs from each treatment group (Table 4). At all time points, the lungs of

TABLE 3.—Bronchoalveolar lavage lung injury parameters

Treatment	LDH (U/L)	Albumin (mg/ml)
24 hr		
PBS	49.9 ± 2.9	0.11 ± 0.01
Si	132.6 ± 11.6[a]	0.47 ± 0.13[a]
WF	288.4 ± 44.8[b]	0.86 ± 0.25[a]
1 wk		
PBS	76.3 ± 19.6	0.12 ± 0.01
Si	158.3 ± 28.3[a]	0.23 ± 0.02[a]
WF	163.0 ± 21.6[a]	1.05 ± 0.21[b]
16 wk		
PBS	60.0 ± 3.8	0.16 ± 0.01
Si	128.3 ± 10.1[c]	0.22 ± 0.01[c]
WF	71.0 ± 12.6	0.16 ± 0.02

Note: Values are means ± SE (n ≥ 4); PBS is phosphate-buffered saline control; Si is silica; WF is welding fume.
[a] Significantly greater than PBS at corresponding time point ($p < 0.05$).
[b] Significantly greater than PBS and Si groups at corresponding time point ($p < 0.05$).
[c] Significantly greater than PBS and WF groups at corresponding time point ($p < 0.05$).

TABLE 4.—Lung histopathology scores

Treatment	Bronchiolar epithelial cellular atypia	Alveolar bronchiolo-alveolar hyperplasia	Bronchiolar bronchiolo-alveolar hyperplasia	Lymphoid hyperplasia	Inflammation	Fibrosis
1 wk						
PBS	0.00 ± 0.00	0.00 ± 0.00	0.00 ± 0.00	0.00 ± 0.00	0.00 ± 0.00	0.00 ± 0.00
Si	0.00 ± 0.00	2.50 ± 2.50	0.00 ± 0.00	0.00 ± 0.00	6.00 ± 0.00	2.00 ± 2.00
WF	7.00 ± 0.00	8.00 ± 1.00	0.00 ± 0.00	0.00 ± 0.00	8.00 ± 0.00	0.00 ± 0.00
8 wk						
PBS	0.00 ± 0.00	0.00 ± 0.00	0.00 ± 0.00	0.00 ± 0.00	0.00 ± 0.00	0.00 ± 0.00
Si	0.00 ± 0.00	5.25 ± 0.92[b]	0.00 ± 0.00	4.38 ± 1.46[b]	5.63 ± 0.38[c]	5.25 ± 0.25[c]
WF	1.13 ± 0.66[a]	0.00 ± 0.00	3.13 ± 0.85[a]	0.00 ± 0.00	5.50 ± 0.20[c]	5.00 ± 0.41[c]
16 wk						
PBS	0.00 ± 0.00	0.00 ± 0.00	0.00 ± 0.00	0.00 ± 0.00	0.00 ± 0.00	0.00 ± 0.00
Si	0.00 ± 0.00	6.00 ± 0.20[b]	0.00 ± 0.00	5.88 ± 0.38[b]	5.88 ± 0.13[c]	5.5 ± 0.29[b]
WF	2.88 ± 0.38[a]	0.00 ± 0.00	3.50 ± 0.61[a]	1.25 ± 0.72	4.88 ± 0.31[c]	3.75 ± 0.63[c]
24 wk						
PBS	0.00 ± 0.00	0.00 ± 0.00	0.00 ± 0.00	0.00 ± 0.00	0.00 ± 0.00	0.00 ± 0.00
Si	0.50 ± 0.50	6.38 ± 0.38[b]	0.00 ± 0.00	6.00 ± 0.29[b]	6.63 ± 0.38[c]	5.00 ± 0.00[c]
WF	5.13 ± 0.66[a]	0.00 ± 0.00	5.25 ± 0.14[a]	1.50 ± 1.50	5.13 ± 0.13[c]	5.75 ± 0.25[c]

Note: Values are means ± SE for 1 wk (n = 2) and 8, 16, and 24 wk (n = 4); statistical analysis performed for 8,16, and 24 wk; PBS is phosphate-buffered saline control; Si is silica; WF is welding fume.

[a] Significantly greater than PBS and Si groups at corresponding time point ($p < 0.05$).

[b] Significantly greater than PBS and WF groups at corresponding time point ($p < 0.05$).

[c] Significantly greater than PBS group at corresponding time point ($p < 0.05$).

the control mice appeared normal although bronchiolar BAH was found in control mice at the 48 week time point (data not shown). Pulmonary exposure to WF at 1 week was associated with a marked, multifocal and coalescent, peribronchiolar lymphogranulomatous response (lymphocytes and epitheloid macrophages predominated; neutrophils were not a major component). The normal architecture of the pulmonary tissue adjacent to affected bronchioles was largely effaced, and there was intrahistiocytic accumulation of brown material consistent with WF exposure. Proliferative changes in the alveolar region at 1 week consisted of moderate alveolar BAH. Proliferative changes in the bronchioles consisted of bronchiolar epithelial hyperplasia with atypia. The alveolar BAH was most prominent at the periphery of the peribronchiolar inflammatory response while bronchiolar epithelial hyperplasia with atypia involved the epithelium lining bronchioles (Figure 1A & B).

At 8 weeks postexposure, restoration of pulmonary architecture was observed in the WF-exposed mice. However, histiocytic inflammation, bronchiolar cellular atypia, and proliferative tissue alterations persisted. At 8 weeks, peribronchiolar proliferative lesions in WF-exposed mice were predominantly bronchiolar BAH rather than alveolar BAH observed at 1 week. Alveolar septal fibrosis was observed in all WF-exposed mice at 8 weeks but was generally mild. At 16 and 24 weeks postexposure, findings in WF-exposed mice were similar to those seen at 8 weeks. At both 16 and 24 weeks, bronchiolar cellular atypia (Figures 1C & D) and bronchiolar BAH (Figure 2A&B) were seen in all WF-exposed mice and in none of the controls. Persistent histiocytic inflammation was generally near the bronchioles. The histiocytic aggregates contained brown-black particulate consistent with WF particles. At 48 weeks after exposure, focal severe alveolar epithelial cell hypertrophy and hyperplasia were seen in one of the WF-exposed mice. A papillary bronchoalveolar adenoma was observed in the other WF-exposed mouse (data not shown). Foci of fibrosis were generally mild at this time point.

The inflammatory response to silica at 1 week was histiocytic and suppurative (comprised of macrophages and neutrophils) and distributed multifocally within the lung. Epithelial proliferative responses were mild and multifocal but included proliferative bronchiolitis obliterans, involving the terminal bronchioles and alveolar ducts, in one mouse. At 8 weeks, hyperplasia of perivascular and bronchus-associated lymphoid tissue was a prominent finding in 3 of the 4 silica-exposed mice. Alveolar BAH and alveolar septal fibrosis were seen in all silica-exposed mice. The alveolar BAH was typical of silicosis and often involved increased numbers of discrete hypertrophied alveolar type II cells and in 3 of 4 mice, alveolar lipoproteinosis was observed.

In silica-exposed mice at 16 and 24 weeks postexposure, bronchiolar BAH was not observed. Similarly, bronchiolar cellular atypia was noted in only one mouse. The inflammatory response to silica continued to be histiocytic and suppurative with a significant neutrophilic component (Figure 3A). Lymphoid hyperplasia was a variable finding in the WF-exposed lung, while lymphoid hyperplasia was seen in all silica-exposed lungs at 24 weeks after exposure. Alveolar BAH was a consistent response in all silica-exposed mice (Figure 3B & C). Increased numbers of large, alveolar epithelial cells were consistent with alveolar epithelial cell hypertrophy as well as hyperplasia. These hypertrophied type II cells were most frequently present in increased numbers without forming a contiguous layer, although this was sometimes observed. Consistent with the alveolar BAH, the product of alveolar type II cells, lipoprotein also appeared to increase, with alveolar lipoproteinosis observed in all but one silica-exposed animal. Alveolar epithelial cell hypertrophy and hyperplasia in silica-exposed mice at 48 weeks postexposure was similar to that seen at earlier time points and foci of fibrosis were generally mild.

DISCUSSION

This study presents an assessment of the potential of MMA-SS WF to induce lung inflammation and injury in A/J

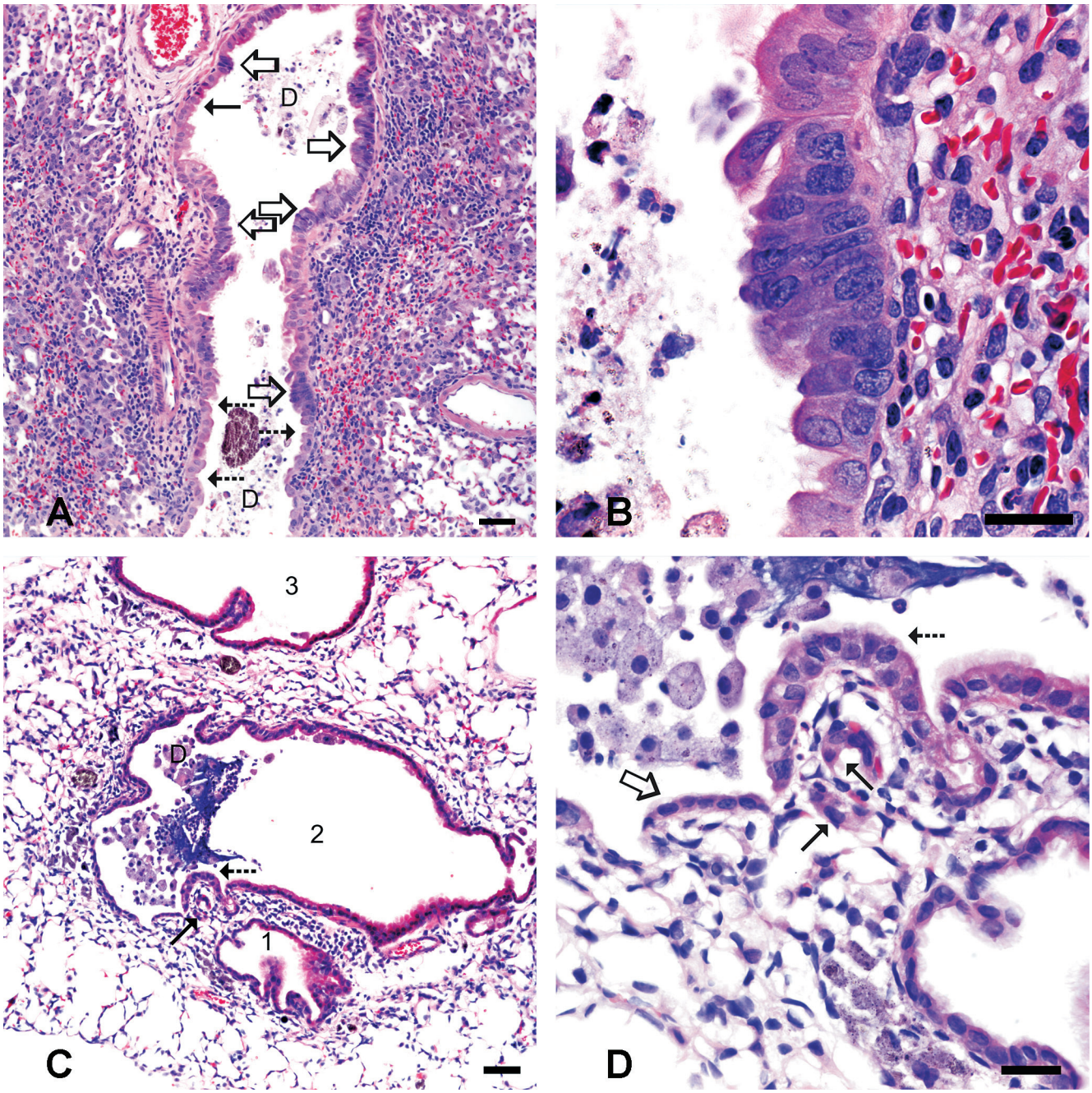

FIGURE 1.—Photomicrographs of bronchiolar epithelial regenerative hyperplasia and cellular atypia in WF-exposed mice. (A) Low magnification image of mouse lung tissue 1 week postexposure. Some unaffected bronchiolar epithelium remains (solid arrow). Increased cytoplasmic basophilia, large round to oval nuclei, irregularly placed nuclei and an increased numbers of non-ciliated airway epithelial cells are features of the hyperplastic airway epithelial response to injury at 1 week after exposure (dashed arrow). In some foci, changes in the epithelium are more pronounced and classified as cellular atypia (open arrows) which at 1 week was characterized as a multilayered columnar epithelium with intense cytoplasmic basophilia, irregulary placed nuclei, and a high nuclear to cytoplasmic ratio. Cellular debris (D) was noted in the airway lumen (bar is 50 microns). (B) A higher magnification of a focus of cellular atypia from the previous photomicrograph (bar is 20 microns). (C) Low magnification image of mouse lung tissue 16 weeks post-exposure to WF. Cross-sections of three bronchioles labeled 1, 2, and 3. In addition to these bronchioles, tube-like structures lined by bronchiolar epithelium (solid arrows) are adjacent to bronchiole 2. The lumen of bronchiole 2 contains abundant debris (D) comprised of macrophages, neutrophils, cholesterol clefts and mucous. A focus of mild cellular atypia (dashed arrow) is identified at this magnification by the increased cytoplasmic basophilia and cell size (bar is 50 microns). (D) At higher magnification the focus of cellular atypia (dashed arrow) is characterized by increases in both nuclear size and cytoplasmic volume, cytoplasmic basophilia, and variations in nuclear location within the cell resulting in a dramatic increase in cell size relative to the adjacent more normal epithelium (open arrow). The small tube-like structures (solid arrows) are similar in size to adjacent alveoli and may represent either embryonic tube-like structure or bronchiolization of peribronchiolar alveolar septa.

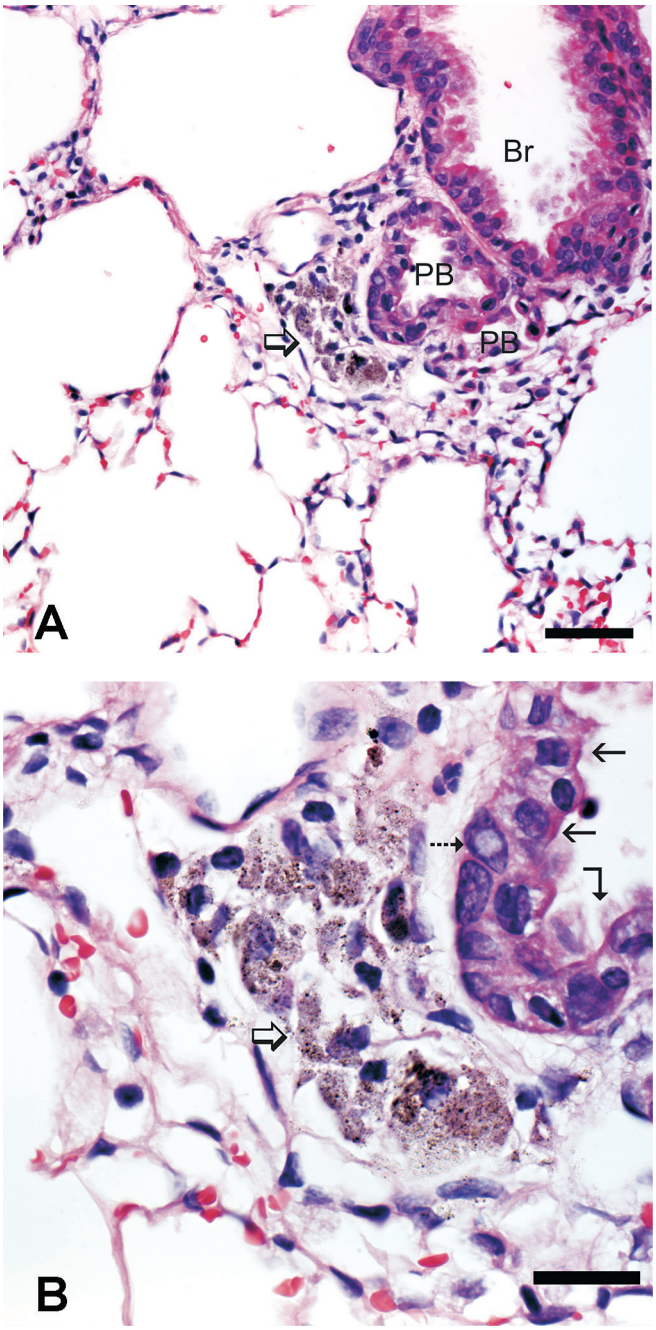

FIGURE 2.—Photomicrograph of bronchiolar epithelial hyperplasia adjacent to a small bronchiole at 16 weeks in a WF-exposed mouse. (A) Two tube-like peribronchiolar structures (PB) are adjacent to a small bronchiole (Br). One of these structures is entirely lined by mildly flattened bronchiolar epithelium with mild karyomegaly and the other structure is partially lined by a flattened bronchiolar epithelium and partially lined by alveolar epithelium. An aggregate of macrophages (open arrow) adjacent to these structures contains cytoplasmic pigment consistent with WF particles (bar is 50 microns). (B) A higher magnification of the aggregate of macrophages (open arrow) and bronchiolization of tube like-structure with atypical bronchiolar epithelium characterized by apical nuclear location (solid straight arrows), nuclear pseudoinclusion (dashed arrow), and cilia (angle arrow). Bar is 20 microns.

mice, a lung tumor susceptible mouse strain. Crystalline silica, or α-quartz, served as a comparative pneumotoxic particle control. WF-induced lung inflammation and damage has been widely investigated using other rodent models (Antonini

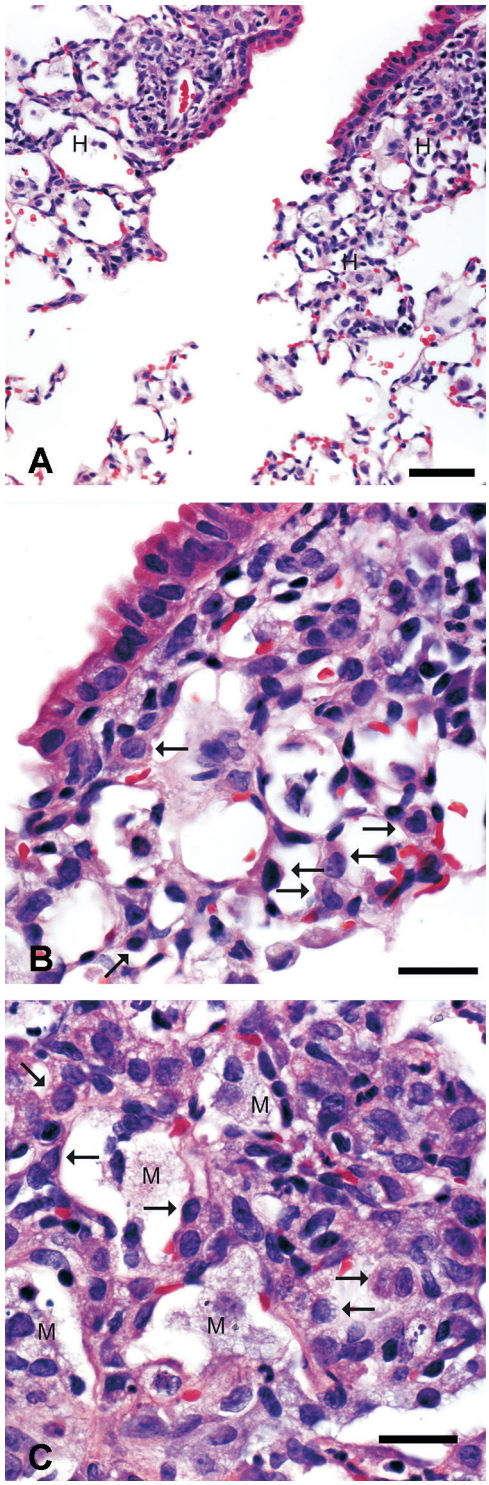

FIGURE 3.—Photomicrographs of a terminal bronchiole and adjacent alveoli in silica-exposed mice at 16 weeks. (A) Morphologic changes are characterized by histiocytic and suppurative inflammation (H), which is generally localized to peribronchiolar alveoli (bar is 50 microns). (B) In a higher magnification of peribronchiolar alveoli, lining cells consistent with alveolar type II cells (arrows) are abundant and have foamy eosinophilic cytoplasm which projects from the alveolar septa. These changes are consistent with alveolar epithelial cell hypertrophy and hyperplasia (bar is 20 microns). (C) A different alveolar region from the same mouse demonstrating marked alveolar epithelial cell hypertrophy and hyperplasia (arrows) with associated histiocytic and suppurative inflammation of alveoli characterized by increased numbers of macrophages (M) and lesser numbers of neutrophils (bar is 20 microns).

et al., 1996, 1997). However, the A/J mouse model will allow for a better understanding of spontaneous or particle-induced neoplastic changes that may occur in the lung. This mouse model is of special interest due to existing similarities with lung adenocarcinoma development in humans. As mentioned, mice develop lung tumors that resemble human lung adenocarcinomas in their anatomy, histogenesis, and molecular features (Malkinson, 1998). For example, the *Pas1* locus, a major mouse lung tumor susceptibility locus first mapped in A/J mice, appears to have a human counterpart which also conveys susceptibility to the development of human lung adenocarcinoma (Dragani et al., 2000). These data suggest that findings in the A/J mouse lung tumor model will have direct relevance to humans and the present study will serve as an initial step toward further characterization of the carcinogenic potential of WF.

An important histopathological finding in this study was the presence of bronchiolo-alveolar hyperplasia, including alveolar BAH and bronchiolar BAH. In this study, silica exposure produced a form of alveolar BAH sometimes called hyperplasia and hypertrophy of alveolar epithelium, a well-characterized response to silica exposure in the rat (Miller and Hook, 1990). Suggesting a potential sensitivity of the A/J strain, alveolar BAH is generally not described in the silica-exposed mouse (Saffiotti et al., 1994). While often subtle and most frequently characterized by increased numbers of discrete cuboidal epithelial cells rather than the contiguous single layer of hypertrophied alveolar cells typical of alveolar BAH in the mouse, the change within the alveolar epithelium was distinctive. In addition, the associated presence of lipoproteinosis supported increased secretion of the product of alveolar type II cells, surfactant. Although macrophage death may also cause lipoproteinosis, this response in a rat model of silicosis has been attributed to hypertrophy and hyperplasia of alveolar type II cells (Miller et al., 1990). In contrast, WF-exposed mice developed bronchiolar BAH. In some cases, the bronchiolar BAH resembled fetal-like tubule formation, which can be a bronchiolar regenerative response to toxic injury (Dixon et al., 1999). Bronchiolo-alveolar hyperplastic lesions, particularly atypical adenomatous hyperplasia, are the earliest lesion seen during the sequential development of lung cancer in *K-ras*^{LA} mutant mice and these lesions are generally considered both proliferative and metaplastic (Johnson et al., 2001; Ress et al., 2003).

Bronchiolar epithelial cellular atypia was another important histopathological finding in this study. Primarily associated with WF exposure, but not silica, this cellular atypia was characterized by variation in cellular/nuclear size and shape of lining cells, increased nuclear basophilia, and increased nuclear invagination. These findings when combined with hyperplasia have sometimes been classified as dysplasia (Dungworth et al., 2001). However, to prevent conflict, the term cellular atypia was used in this study because a definitive preneoplastic change could not be confirmed. The cellular atypia observed in the bronchiolar epithelium after WF exposure occurred early, at the 1-week time point, which is consistent with a somewhat disorganized repair. However, a subsequent increase in atypical epithelial changes at later time points, observed in the WF-exposed mice only, suggests a need for further study.

The BAL analysis also revealed a differential progression from initial injury between the WF and silica-exposed animals. At the earlier time points, lung injury and inflammation were elevated after exposure to both WF and silica. However, in contrast to the chronic injury and inflammatory profile (largely neutrophilic) observed in silica-exposed mice, the WF group lacked this response and, by 16 weeks, had normal BAL neutrophils, lung permeability (albumin), and cytotoxicity (LDH) profiles. Persistent, largely interstitial, histiocytic inflammation (neutrophils were not a major component), not evidenced by the BAL, was observed histopathologically in the WF-exposed mice. Some studies suggest that chronic inflammation, attributable to activated macrophages, may lead to cancer (Marx, 2004). Whether the varying manifestations of persistent lung inflammation, in the WF or silica-exposed mice, lend an inference to a potential preneoplastic change remains unknown.

The limitations of the present study need to be addressed to thoroughly plan for future research involving this A/J mouse model. First, dosing parameters may need to be adjusted. The two particulates were compared based on equal mass as a starting point. A single bolus dose of approximately 1 mg per particle was used, which may not have been the most applicable approach due to differences in particle surface area, size and/or number. In subsequent studies, a lower bolus dose and more frequent administration of the particulate over time is appropriate.

Second, cancer bioassays typically involve experimental groups on the order of 50 animals per group, which aids in achieving statistical significance of treated groups over the background tumor incidence in untreated A/J mice. Larger scale studies are being planned that will address this issue. In addition, a highly potent positive tumorigenic control, such as urethane, Cr, and/or Ni subsulfide, should be used in these future studies.

Lastly, WFs differ in their metal composition, making it important to examine potential carcinogenic properties of various types. Stainless steel electrodes used during MMA or gas metal arc (GMA) welding, generate fumes containing carcinogenic Cr and Ni. Indeed, these fumes have been shown to be toxic and mutagenic to mammalian cells (Hedenstedt et al., 1977; Maxild et al., 1978). On the other hand, mild steel (MS) fumes contain abundant iron without Cr or Ni. However, MS fumes have been linked to an increased cancer risk as reported in some studies (Moulin et al., 1993; Danielsen et al., 1993). Of interest, previous data showed the soluble fraction of MMA-SS, which is abundant in Cr, generated free radicals and caused significant lung macrophage toxicity (Antonini et al., 1999; Taylor et al., 2003). This implies that Cr may play a role in the increased lung cancer risk of welders; although, to date this has not been proven (Langard, 1994). In addition to MMA-SS WFs, GMA-SS and GMA-MS will be examined in future studies, as well as insoluble and soluble Cr.

In conclusion, animal studies are certainly needed to determine if exposure to WF alone causes lung cancer. Based on the evidence in this pilot study, it can not be concluded that MMA-SS WF induces neoplastic changes in the lungs of A/J mice. However, it can be concluded that MMA-SS WF induces atypical hyperplastic changes that do not occur with silica over a 48-week time course. Seemingly,

these changes progress in the absence of significantly elevated BAL lung parameters indicative of lung inflammation and injury. These findings support the need to further investigate WF as a possible carcinogenic particulate. Studies are currently underway to determine relative potencies, albeit inflammatory or carcinogenic, of different WFs in A/J mice.

ACKNOWLEDGMENTS

The authors would like to thank Dr. Michael Kashon for his help with the statistical analyses. The authors also would like to acknowledge Dr. Lyndell Millecchia for her critical review and editorial comments regarding the manuscript.

REFERENCES

Antonini, J. M. (2003). Health effects of welding. *Crit Rev Toxicol* **33**, 61–103.

Antonini, J. M., Lawryk, N. J., Krishna Murthy, G. G., and Brain, J. D. (1999). Effect of welding fume solubility on lung macrophage viability and function *in vitro*. *J Toxicol Environ Health Part A* **58**, 343–63.

Antonini, J. M., Krishna Murthy, G. G., and Brain, J. D. (1997). Responses to welding fumes: lung injury, inflammation, and the release of tumor necrosis factor-alpha and interleukin 1β. *Exp Lung Res* **23**, 205–27.

Antonini, J. M., Krishna Murthy, G. G., Rogers, R. A., Albert, R., Ulrich, G. D., and Brain, J. D. (1996). Pneumotoxicity and pulmonary clearance of different welding fumes after intratracheal instillation in the rat. *Toxicol Appl Pharmacol* **140**, 188–99.

Becker, N. (1999). Cancer mortality among arc welders exposed to fumes containing chromium and nickel. *J Occup Environ Med* **41**, 294–303.

Danielsen, T. E., Langard, S., and Andersen, A. (2000). Incidence of cancer among welders and other shipyard workers with information on previous work history. *J Occup Environ Med* **42**, 101–9.

Danielsen, T. E., Langard, S., Andersen, A., and Knudsen, O. (1993). Incidence of cancer among welders of mild steel and other shipyard workers. *Br J Ind Med* **50**, 1097–103.

Dixon, D., Herbert, R. A., Sukks, R. C., and Boorman, G. A. (1999). Lungs, pleura and mediastinum. In Pathology of the Mouse (R.R. Maronpot, G. A Boorman, and B. W. Gaul, eds.). Cache River Press, Vienna, IL.

Dragani, T. A., Hirohashi, S., Juji, T., Kawajiri, K., Kihara, M., Ono-Kihara, M., Manenti, G., Nomoto, T., Sugimura, H., Genka, K., Yokota, J., Takahashi, T., Mitsudomi, T., and Nagao, M. (2000). Population-based mapping of pulmonary adenoma susceptibility 1 locus. *Cancer Res* **60**, 5017–20.

Dungworth, D. L., Rittinghausen, S., Schwartz, L., Harkema, J. R., Hayashi, Y., Kittel, B., Lewis, D., Miller, R. A., Mohr, U., Morgan, K. T., Rehm, S., and Slayter, M. V. (2001). Respiratory system and mesothelium. In International Classification of Rodent Tumors: The Mouse (U. Mohr, P. Greaves, N. Ito, C. C. Capen, J. F. Hardisty, P. H. Long, D. L. Dungworth, Y. Hayashi, and G. Krinke, eds.). WHO IARC, Springer, Berlin, Germany.

Gariboldi, M., Manenti, G., Canzian, F., Falvella, F. S., Radice, M. T., Pierotti, M. A., Della Porta, G., Binelli, G., and Dragani, T. A. (1993). A major susceptibility locus to murine lung carcinogenesis maps on chromosome 6. *Nature Genet* **3**, 132–6.

Hansen, K. S., Lauritsen, J. M., and Skytthe, A. (1996). Cancer incidence among mild steel and stainless steel welders and other metal workers. *Am J Ind Med* **30**, 373–82.

Hedenstedt, A., Jenssen, D., Lidesten, B., Ramel, C., Rannug, U., and Stern, R. M. (1977). Mutagenicity of fume particles from stainless steel welding. *Scand J Work Environ Health* **3**, 203–11.

Hubbs, A. F., Castranova, V., Ma, J. Y., Frazer, D. G., Siegel, P. D., Ducatman, B. S., Grote, A., Schwegler-Berry, D., Robinson, V. A., Van Dyke, C., Barger, M., Xiang, J., and Parker, J. (1997). Acute lung injury induced by a commercial leather conditioner. *Toxicol Appl Pharmacol* **143**, 37–46.

International Agency for Research on Cancer (1990). Chromium, nickel, and welding. In IARC Monographs on the Evaluation of Carcinogenic Risks to Humans, Vol. 49, pp. 447–525. WHO IARC, Geneva, Switzerland.

Johnson, L., Mercer, K., Greenbaum, D., Bronson, R. T., Crowley, D., Tuveson, D., and Jacks, T. (2001). Somatic activation of the K-ras oncogene causes early onset lung cancer in mice. *Nature* **410**, 1111–6.

Langard, S. (1994). Nickel-related cancer in welders. *Sci Total Environ* **148**, 303–09.

Malkinson, A. M. (1989). The genetic basis of susceptibility to lung tumors in mice. *Toxicology* **54**, 241–71.

Malkinson, A. M. (1998). Molecular comparison of human and mouse pulmonary adenocarcinomas. *Exp Lung Res* **24**, 541–55.

Manenti, G., Gariboldi, M., Elango, R., Fiorino, A., De Gregorio, L., Falvella, F. S., Hunter, K., Housman, D., Pierotti, M. A., and Dragani, T. A. (1996). Genetic mapping of a pulmonary adenoma resistance locus (*Par1*) in mouse. *Nature Genet* **12**, 455–7.

Manenti, G., Stafford, A., De Gregorio, L., Gariboldi, M., Falvella, F. S., Avner, P., and Dragani, T. A. (1999). Linkage disequilibrium and physical mapping of *Pas1* in mice. *Genome Res* **6**, 639–46.

Marx, J. (2004). Inflammation and cancer: the link grows stronger. *Science* **306**, 966–68.

Maxild, J., Andersen, M., Kiel, P., and Stern, R. M. (1978). Mutagenicity of fume particles from metal arc welding on stainless steel in the salmonella/microsome test. *Mutat Res* **56**, 235–43.

Meuwissen, R., and Berns, A. (2005). Mouse models for human lung cancer. *Genes Dev* **19**, 643–64.

Miller, B. E., Bakewell, W. E., Katyal, S. L., Singh, G., and Hook, G. E. (1990) Induction of surfactant protein (SP-A) biosynthesis and SP-A mRNA in activated type II cells during acute silicosis in rats. *Am J Respir Cell Mol Biol* **3**, 217–26.

Miller, B. E., and Hook, G. E. (1990). Hypertrophy and hyperplasia of alveolar type II cells in response to silica and other pulmonary toxicants. *Environ Health Perspect* **85**, 5–23.

Moulin, J. J. (1997). A meta-analysis of epidemiologic studies of lung cancer in welders. *Scand J Work Environ Health* **23**, 104–13.

Moulin, J. J., Wild, P., Haguenoer, J. M., Faucon, D., DeGaudemaris, R., Mur, J. M., Mereau, M., Gary, Y., Toamain, J. P., Birembaut, Y., Blanc, M., Debiolles, M. P., Jegaden, D., Laterrière, B., Léonard, M., Marini, F., Massardier, C., Moulin, M., Reure, M., Rigal, L., Robert, G., and Viossat, M. (1993). A mortality study among mild steel and stainless steel welders. *Br J Ind Med* **50**, 234–43.

Rao, G. V. S., Tinkle, S., Weissman, D. N., Antonini, J. M., Kashon, M. L., Salmen, R., Batelli, L. A., Willard, P. A., Hoover, M. D., and Hubbs, A. F. (2003). Efficacy of a technique for exposing the mouse lung to particles aspirated from the pharynx. *J Toxicol Environ Health Part A* **66**, 1441–5.

Ress, N. B., Chou, B. J., Renne, R. A., Dill, J. A., Miller, R. A., Roycroft, J. H., Hailey, J. R., Haseman, J. K., and Bucher, J. R. (2003). Carcinogenicity of inhaled vanadium pentoxide in F344/N rats and B6C3F$_1$ mice. *Toxicol Sci* **74**, 287–96.

Saffiotti, U., Daniel, L. N., Mao, Y., Shi, X., Williams, A. O., and Kaighn, M. E. (1994). Mechanisms of carcinogenesis by crystalline silica in relation to oxygen radicals. *Environ Health Perspect* **102**(Suppl 10), 159–63.

Shimkin, M.B., and Stoner, G.D. (1975). Lung tumors in mice: application to carcinogenesis bioassay. *Adv Cancer Res* **21**, 1–58.

Simonato, L., Fletcher, A. C., Andersen, A., Anderson, K., Becker, N., Chang-Claude, J., Ferro, G., Gérin, M., Gray, C. N., Hansen, K. S., Kalliomäki, P. L., Kurppa, K., Långard, S., Merló, F., Moulin, J. J., Newhouse, M. L., Peto, J., Pukkala, E., Sjögren, B., Wild, P., Winkelmann, R., and Saracci, R. (1991). A historical prospective study of European

stainless steel, mild steel and shipyard welders. *Br J Ind Med* **48**, 145–54.

Steenland, K., Beaumont, J., and Elliot, L. (1991). Lung cancer in mild steel welders. *Am J Epidemiol* **133**, 220–9.

Sterling, T. D., and Wenkham, J. J. (1976). Smoking characteristics by type of employment. *J Occup Med* **18**, 743–54.

Taylor, M. D., Roberts, J. R., Leonard, S. S., Shi, X., and Antonini, J. M. (2003). Effects of welding fumes of differing composition on free radical production and acute lung injury and inflammation in rats. *Toxicol Sci* **75**, 181–91.

Van Zandwijk, N., Mooi, W. J., and Rodenhuis, S. (1995). Prognostic factors in NSCLC. Recent experiences. *Lung Cancer* **12**(Suppl 1), S27–33.

Zeidler, P., Hubbs, A., Battelli, L., and Castranova, V. (2004). Role of inducible nitric oxide synthase-derived nitric oxide in silica-induced pulmonary inflammation and fibrosis. *J Toxicol Environ Health Part A* **67**, 1001–26.